

Pocket Milling of AISI 1045 Steel using Abrasive Water Jet Machining by Varying Contours

VISHNUJA UMAPATHY*, BHASKAR GOVINDASWAMY BHAVANI

Department of Production Technology, Madras Institute of Technology, Anna University, Chennai, 600 044, India

Abstract: Abrasive water jet machining (AWJM) is an innovative machining technology recognized for cutting tougher materials smoothly. This study investigates the significance of AWJM parameters on surface roughness (SR) and material removal rate (MRR); while machining AISI1045 medium carbon steel. Pocket milling has been done on the material; pockets of definite size/specifications are machined and associated MRR and SR are investigated. The Input parameters considered are Standoff distance (SOD), Cutting feed, Pressure. Experimental parameters are analyzed as per Taguchi method (DOE). The interaction effects of input process parameters are studied through 3D contour plots. ANOVA is used to determine the influencing parameter, and it has been verified that the ideal combination of Taguchi process parameters satisfies the actual machining of material.

Keywords: AWJM, AISI 1045, pocket milling, L9 orthogonal array, ANOVA, MRR, SR

1. Introduction

In the conventional milling process, a rotary cutter is used to remove material to form complex shapes and components. However, while machining intricate internal primitive shapes. The rotary cutter acts as a limitation as edges need a minimum radius of curvature. Sharp edges also cause distortion and even cracking. Hence it is necessary to go for non-contact (tool - work piece) machining such as beam process/flexible jet machining. AWJM is unconventional machining processes where abrasives are propelled by water at a high-velocity impinge the work piece. This action causes precise material removal due to impact erosion with minimal heat generation. This makes the process suitable for heat sensitive and brittle materials [1]. The high pressure of the fluid results in erosion of local material removal on the surface. This effect can be compounded by addition of abrasives in the jet. AWJM process carries many advantages compared to conventional machining processes due to its nature of cutting. Since there is a negligible heating, heat affected zones are minimal. This results in minimal thermal distortion. As a result, machining defects are reduced to a great extent. Burr formation does not occur precisely in most cases. However, since the tool does not contact the work-piece directly, tool wear is very low. Additionally, tool breakage does not happen. This results in sustained machining lower operating costs, and more accurate work-pieces.

Due to the versatility of the AWJM process, recent developments in the field have enabled various machining operations to be carried out. In addition to cutting, turning, threading, slotting and milling operations can be carried out. Pocket milling is the process where shapes are cut on the work-piece surface. In this milling operation, the water jet does not cut a through hole in the work-piece; instead, the machining is focused on material removal on the surface. Pocket milling is used widely to machine parts for automotive and other complicated industrial components. Pocket milling using abrasive water jet machine has been explored by researchers recently due to its evident advantages. Work has been done on materials like titanium alloys, Aluminum 8011, Inconel 718 and brass.

Based on the studies of optimizations for AWJM process parameters while cutting mild steel using Taguchi technique and Anova it is possible to decide the influencing process parameters [1]. Interaction effects of input process parameters are seen by 3D surface plots. Transverse speed is the most important element determining surface roughness, whereas SOD and abrasive flow rate are the most important factors influencing kerf taper angle.

*email: vishnujaumapathy3@gmail.com



As per the blind pocket milling on Titanium alloy (Ti-6Al-4V), a rapid calibration method is used to optimize the pocket cutting in real-time [2]. As per the investigation on machining of high carbon high chromium steel material with variations on AWJM parameters with respect to MRR and SR. it finds that optimal combination of parameters that meet the real machining parameters of AISI D3 in actual practice [3].

Similarly optimization of process parameters for cutting elliptical pockets on AISI 304 materials, shows further percentage utilization of tool is developed to compare the different tool path strategies and aspect ratios [4]. The impact of step over and traverse speed on pocket milling of Inconel 825 material are affected by the Process parameters are performed in two strategies namely hatch strategy and Spiral strategy [5]. As per the building a novel numerical cutting model that incorporates fluid structure interaction. The mechanical and thermal impacts of the water jet on chip formation and fragmentation are ensured by this model, as illustrated by the numerical model [6].

The general process for blind pocket milling with AWJM on SS304 material. Pocket milling is carried out when the pressure of the jet is reduced, and the standoff distance is increased [7]. This ensures that material removal occurs on the surface instead of causing a through hole. The process parameters have been selected and an ANOVA analysis is carried out to ensure experiments are conducted in a systematic way. The impact of standoff distance and traverse speed has been discussed in detail. Tool traverse path and its effect on output parameters such as surface roughness have also been discussed. Experiments on dense silicon nitride materials by using AWJM. In this work silicon carbide grits (80 B. S) instead of garnet sand was used. Surface roughness of silicon nitride has been calculated [8].

As per the modeled the multiple particle impact on the erosion behaviour of titanium alloy in AWJM using FEA [9]. Author concluded experiments on AISI H13 die steel based on RSM by using central composite design to find significant parameter for surface roughness [10]. As per the investigation on abrasive recycling with and without screening of used abrasives. Recycled abrasives reduces kerf taper through improving the cut of the surface [11]. Developed a hybrid approach for selection of optimal process parameters in AWJM. This model forecasts the depth of cut for each given process parameter combination [12].

As per the experiments in rectangular pocket milling on C-37 steel by using AWJM. The depth of the pocket, the MRR, the erosion rate, and the depth of material removal per machining cycle all varied significantly [13]. Based on the studied machining parameters for processing metallic coated steel sheet with good kerf quality. Empirical models for kerf geometry are predicted [14]. The process for Inconel 718 material with variations introduced due to the mechanical properties of the material used [15]. Studies on planar surfaces, slots and profiles by using abrasive water jet milling [16]. Studies on deep hole drilling on brass by using AWJM, they found the optimal hole parameter by using grey taguchi and RSM method [17]. The machining process for titanium alloy to the unique mechanical properties of the material namely hardness, the machining parameters are varied [18].

From these observations, it is been observed that standard process parameters have not been optimized for steel materials. This paper aims to provide optimized process parameters for AISI 1045 material by using AWJM. The parameters are to be identified and ANOVA analysis is carried out with respect to output parameters. Further, we also need to study the effect of tool path and other variables on the output parameters.

2. Materials and methods

2.1. Material

AWJM is a non-conventional process and it has a versatile machining process. AWJM uses high-pressure water to create a high-velocity stream with abrasive particles. The AISI 1045 steel was chosen for this investigation because it is frequently utilized in the automobile industry. The composition of AISI 1045 steel has been tested before the experiments and shown in Table 1.

Table 1. AISI 1045 steel chemical composition

S.no	Element	Content (%)
1.	Iron (Fe)	98.98
2.	Carbon (C)	0.420
3.	Manganese (Mn)	0.60
4.	Sulfur (S)	0.050
5.	Phosphorus (P)	0.040

2.2. Experimental setup

For Machining pockets with AISI 1045 steel of 100mm X 30mm with 10mm thickness is used, different shapes like square (15mm X 15mm), rectangle (30mm X 15mm), and circle ($\varnothing 22$) during experimentation. The setup consists of a CNC controlled AWJM machine to carry out the machining process. The machine is manufactured by OMAX Corporation, with a model number of 2626. The studies were conducted using Garnet Abrasive with an 80 mesh size. The unit has an active cutting head and direct drive pump. The cutting head is made up of a mixing chamber for water and 80 mesh abrasive garnet. It has a power capacity of 22KW, 415V, 50 Hz. The nozzle diameter is 70 microns. Jet impingement angle 90° . The cutting area is 1168mm \times 787mm and works envelope with x-y cutting travel of 737mm \times 660mm.



Figure 1. a) Pockets in AISI 1045 with Square, Rectangle, and Circle, b) Abrasive water jet machining set up

2.3. Taguchi and ANOVA method

In this study machining of AISI 1045 by AWJM, three control parameters such as Standoff distance, Cutting feed, Pressure are taken. By using Design of experiments control factors are optimized to L9 Orthogonal array [10,12]. These parameters are used to machine the material. Material removal rate and Surface Roughness are selected as responses. Taguchi DOE uses a 2-step optimization process. The signal-to-noise ratio is utilised in the first phase to find the control parameters that reduce variability. Step 2 determines the elements that have a significant effect on the mean while having a negligible effect on the signal-to-noise ratio [3, 8].

Based on Machine specification and considering the medium carbon steel on the machine the following levels are taken. The three input elements with three levels are recorded in Table 2 based on the trial-and-error approach and literature on various steels.

Table 2. Input parameter level

S.No	Parameters	Level 1	Level 2	Level 3
1	SOD (mm)	1	1.5	2
2	Cutting Feed (mm/Min)	30.60	16.46	9.15
3	Pressure (MPa)	35.163	49.642	59.984

Table 3. MRR and SR experimental results based on L9 orthogonal array

Experiment No	SOD (mm)	Cutting Feed (mm/min)	Pressure (MPa)	MRR (mm ³ /min)	Surface roughness (um)	Kerf ratio(mm)
1	1	30.60	35.163	2.4779	2.05	0.01240
2	1	16.46	49.642	1.0725	2.203	0.00963
3	1	9.15	59.984	0.6805	2.133	0.00734
4	1.5	30.60	49.642	1.67	2.25	0.00965
5	1.5	16.46	59.984	1.0552	2.26	0.00964
6	1.5	9.15	35.163	0.6838	1.993	0.00734
7	2	30.60	59.984	1.8212	2.493	0.01056
8	2	16.46	35.163	1.1197	2.033	0.00873
9	2	9.15	49.642	0.7408	2.076	0.00459

After the Experimental investigation of input Parameters, Different response Parameters like MRR and SR are Calculated and tabulated in Table 3. Surface average roughness is observed by Surfcomer SE1200 (μm) with cut off 0.80mm and M-speed 0.50mm/s along transverse and longitudinal directions to the machined sample.

The material removal rate is calculated by Eq. 1

$$\text{MRR} = \text{Weight difference (mm}^3\text{)}/\text{Time (min)} \quad (1)$$

Kerf taper angle(θ) is calculated by Eq. 2

$$\text{Kerf taper angle } (\theta) = \tan^{-1} (W_t - W_d) / 2t \quad (2)$$

As the Kerf taper ratio is minute, it is negligible.

3. Results and discussions

3.1. Surface roughness parameters through statistical analysis

ANOVA is used to determine the significance of output parameters in relation to input parameters [1]. It uses the sum of squares a mathematical methodology to considerably analyze the variation of control parameters. For determine the importance of input parameters, the F test, p-value based on a 95 percent confidence level ($p < 0.05$), and coefficient R^2 determination are utilised. Stepwise regression analysis is used to eliminate the parameter's insignificant effect. Equation 3 shows a second order regression equation for surface roughness.

$$\text{SR} = 1.368 + 0.0720\text{SOD} + 0.00889\text{CF} + 0.01085\text{P} \quad (3)$$

All exert a positive influence on Surface roughness. A rise in standoff distance will result in diffused beam causing in poor machining; a rise in Pressure with normal Incidence of Jet (90 deg impact) will deflect/rebound causing poor cutting.

Regression Analysis for Surface roughness in Statistical values

$$S = 0.0640728, R\text{-sq} = 89.44\%, R\text{-Sq (adj)} = 83.11\%$$

Regression model (3) indicates low p value ($p < 0.05$) and high F value of 26.74; Table 5 shows that there is only a 0.004% probability that the value will occur owing to noise. Equation 3 evaluates the difference in anticipated and experimental values using the experimental data from Table 3. In terms of surface roughness, the mean absolute error is computed as 0.05. Similarly, R^2_{adj} and R^2 values are 83.11% and 89.44% respectively. The contribution of input parameters is listed in ANOVA Table 5.

Figure 2 shows that Ssurface roughness is more sensitive to feed and pressure. All the three parameters give a positive influence.

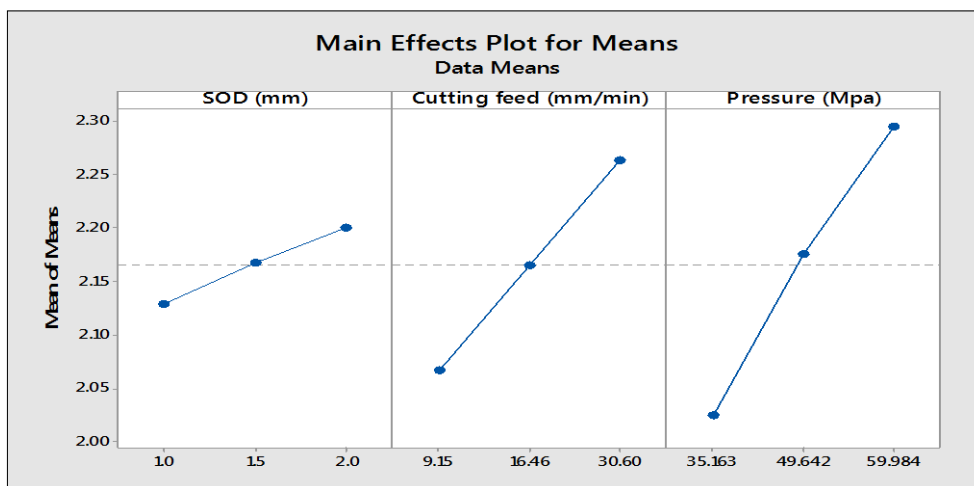


Figure 2. Main effect plot for means (Surface Roughness)

Table 4. Means response table

level	SOD (mm)	Cutting feed (mm/min)	Pressure (MPa)
1	2.129	2.067	2.025
2	2.168	2.165	2.176
3	2.201	2.264	2.295
Delta	0.072	0.197	0.270
Rank	3	2	1

In Taguchi design [10], the mean is the average response for each combination of control factor levels. Figure 2 shows that surface roughness value is minimum when process parameters are SOD as 1mm, Cutting feed as 9.15 mm/min, Pressure as 35.163 MPa. Table 4 reveals that pressure is the most important factor for surface roughness, followed by CF and SOD. Surface roughness rises as pressure increases.

Table 5. Surface roughness analysis of variance table

Source	DF	Seq SS	Adj SS	Seq MS	F -Value	P- value	Contribution (%)
Regression	3	0.173925	0.173925	0.057975	14.12	0.007	89.44
SOD	1	0.007776	0.007776	0.007776	1.89	0.227	4.00
CF	1	0.056371	0.056371	0.056371	13.73	0.014	28.99
P	1	0.109778	0.109778	0.109778	26.74	0.004	56.46
Error	5	0.020527	0.20527	0.004105			10.56
Total	8	0.194452					100.00

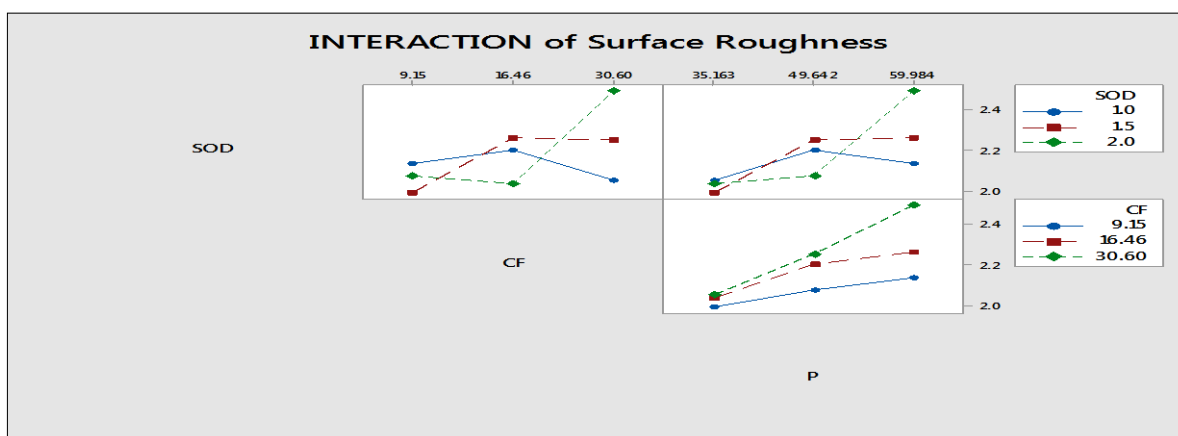


Figure 3. Interaction effect plots of surface roughness

From Figure 3: Interaction effect plots for surface roughness indicates that interactions are present between all the three factors as lines are not parallel. Interaction between SOD and CF indicates that SOD doesn't vary much when compared to CF, as SOD increases cutting feed varies. Interaction between SOD and P indicates that SOD has only minor difference and pressure has maximum variations. Interaction between CF and P indicates that lower pressure the value of R_a is almost the same. Interactions of SOD, P & CF for response Surface roughness are shown. It is perceived that the most governing factor is pressure among all the control factors.

With minimum SOD Surface roughness tends to marginally vary and drop with increased feed. However, with increasing SOD Surface roughness tends to rise with feed. Similar trend is seen with SOD-P interaction, with CF-P interaction, with increasing CF for a given Pressure, Surface roughness increases. Mostly Surface roughness increases with all feeds.

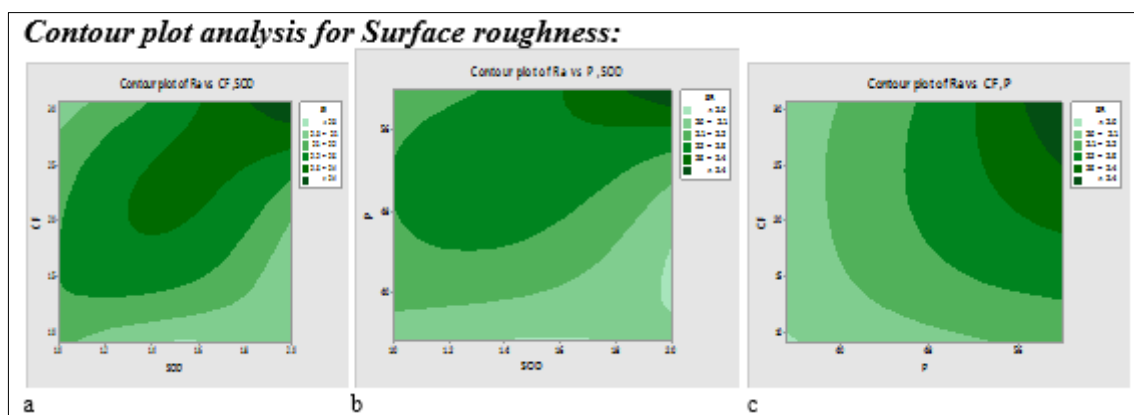


Figure 4a-c. Contour plot analyses for Surface roughness.

- with low CF for all standoff distance surface roughness is low. Increased sod and CF lead to higher order surface roughness.
- with Lower SOD Surface roughness is smaller with increased Pressure Surface roughness increases.
- with low Pressure Surface roughness drops down with Cutting feed, with increased Pressure and CF, Surface roughness increases.

Figure 4a-c depicts the interaction result of two parameters, which are shown graphically using 3D contour plots. Figure 4a depicts standoff distance vs cutting feed while keeping pressure at the mid value of 49.642Mpa. As the standoff distance and cutting feed are reduced, the surface roughness decreases. Surface roughness rises as the Standoff distance and cutting feed are increased. As the standoff distance rises, the driving force of particles impacting with the work-piece rises, resulting in uneven peaks on the machined surface. In Figure 4b shows the combination of Pressure and SOD at constant Cutting feed 36.46(mm/min). Minimum surface Roughness is observed at lower SOD and higher pressure and vice versa. In Figure 4c Cutting feed is shown versus Pressure by keeping Standoff distance as constant at 1.5mm. When the pressure is high and the cutting feed is low, the surface roughness increases, and vice versa.

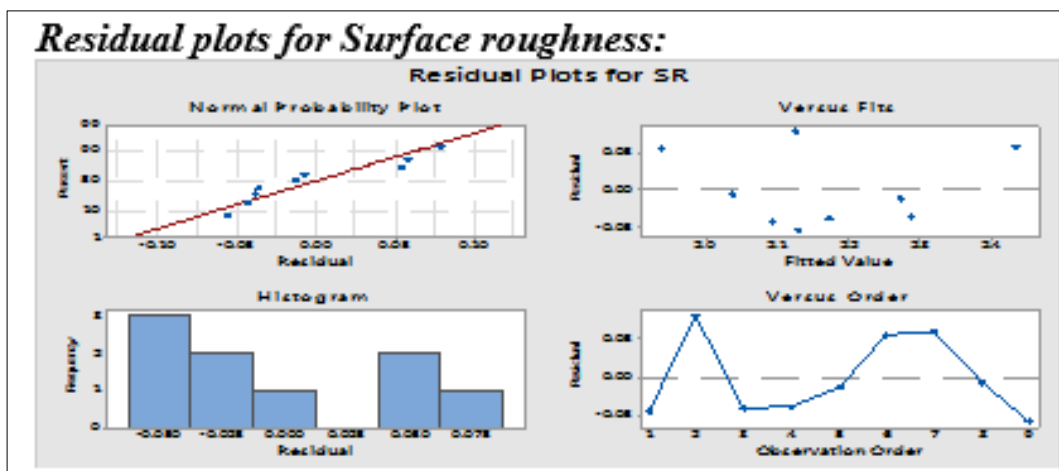


Figure 5. Residual plots for Surface roughness

Surface Roughness is depicted in Figure 5. A normal probability plot, residual vs fits, a histogram for residuals, and residuals versus experimental values are all included in the residual plot. The graphs show that the data follows a normal distribution, with residuals closely following a line in a normal probability graph. Between the measured and estimated values of surface roughness a good correlation is observed.

3.2. Material Removal Rate (MRR) parameters through statistical analysis

Similarly, in the case of MRR, a Mathematical model sum of squares is utilised to examine the modification of control parameters considerably. Table 7 displays the influencing parameters based on their p and F values. The obtained F value of 56.70 and p value 0.001 are indicating that regression model is significant. By using F test and P test based on the confidence level of 95% ($P < 0.05$) the significance of input parameters is investigated and determination of coefficient R^2 . A second –order regression equation for MRR is presented in Equation 4. Table 3 contains the experimental data used to distinguish between observed and predicted values in Equation 4. The mean absolute error (MSE) for MRR is computed as 0.275. Similarly, R^2 adj and R^2 values are 87.68% and 92.30% respectively. Equation 4 shows the regression equation for MRR.

Regression Analysis for MRR in Statistical values

$$S=0.214983 \quad R\text{-Sq}=92.30\% \quad R\text{-Sq(adj)}=87.68\%$$

Regression Equation

$$\text{MRR} = 0.893 - 0.183\text{SOD} + 0.06060 \text{CF} - 0.01028 \text{P} \quad (4)$$

A rise in SOD and P leads to a drop-in material removal rate. A rise in SOD, a diffused beam and increasing Pressure can lead to drop-in material removal rate. Both standoff distance and pressure have negative influence on MRR.

Figure 6 above shows that MRR value is high when the process parameters are SOD 1mm, cutting feed 30.60 mm/min, Pressure 35.163Mpa. Table 6 below shows that Cutting feed has the most significant factor for surface roughness than SOD and Pressure. As the Cutting feed increases, MRR maximizes. As Pressure and SOD decreases MRR increases.

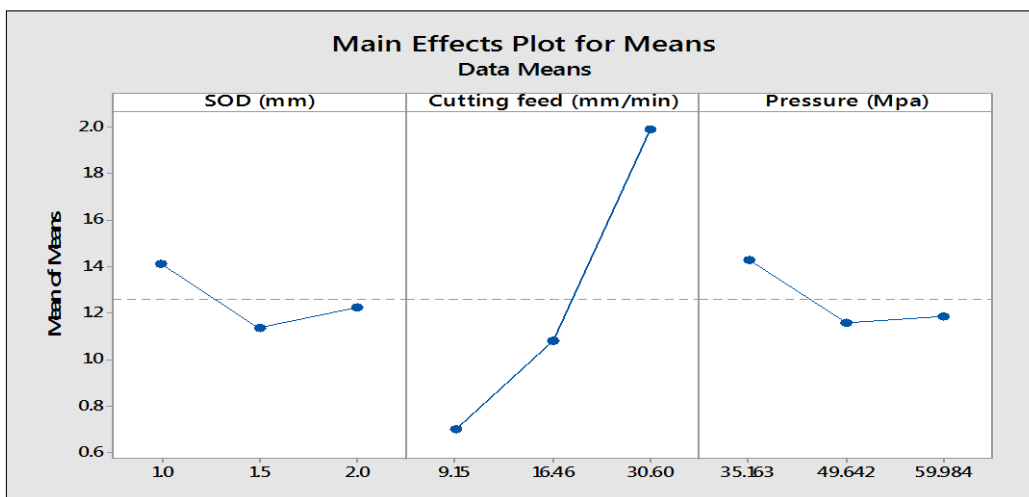


Figure 6. Main effect plot for means (MRR)

Table 6. Response table for means (MRR)

Level	SOD (mm)	Cutting Feed (mm/min)	Pressure (Mpa)
1	1.4103	0.7017	1.4271
2	1.1363	1.0825	1.1611
3	1.2272	1.9897	1.1856
Delta	0.2740	1.2880	0.2660
Rank	2	1	3

Table 7. Analysis of variance table for MRR

Source	DF	Seq SS	Adj SS	Seq MS	F-Value	P -Value	Contribution (%)
Regression	3	2.76938	2.76938	0.92313	19.97	0.003	92.30
SOD	1	0.05027	0.05027	0.05027	1.09	0.345	1.68
CF	1	2.62045	2.62045	2.62045	56.70	0.001	87.33
P	1	0.09866	0.09866	0.09866	2.13	0.204	3.29
Error	5	0.23109	0.23109	0.04622			7.70
Total	8	3.00047					100.00

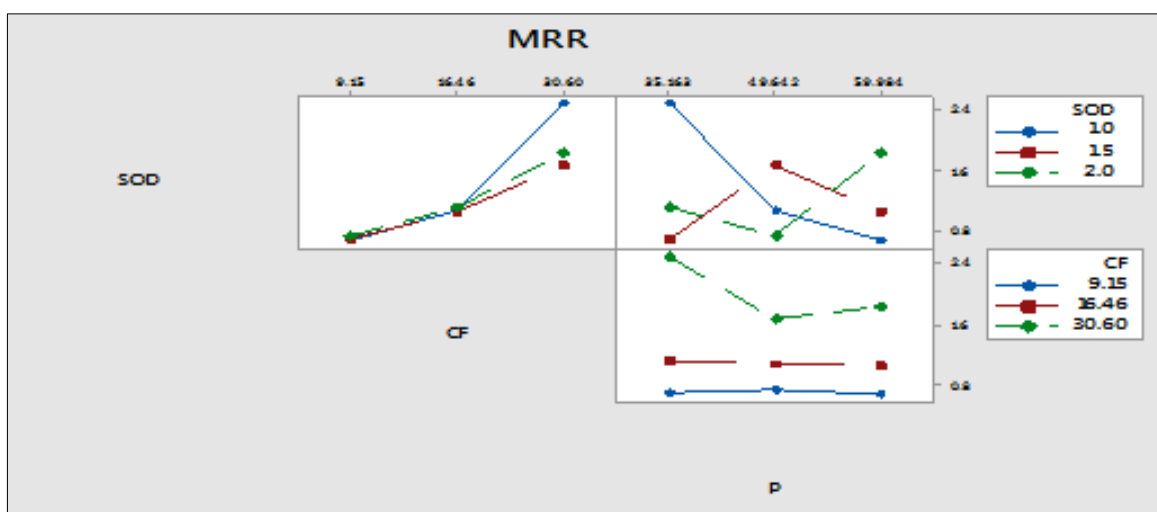


Figure 7. Interaction plots of MRR

Figure 7 SOD - CF interaction low sod with CF material removal rate increases, with 1.5 and 2mm SOD mixed mode of interaction can be seen.

SOD - P interaction minimum SOD with minimum material removal rate drops down, with higher SOD material removal rate tends to rise with increased Pressure.

CF- P interaction up to medium CF material removal rate increases with P with higher CF material removal rate tends to drop down with Pressure.

Figure 7 above shows the interaction plots of MRR with Input parameters. Interaction between CF and SOD indicates that SOD doesn't vary much when compared to cutting feed. As the SOD increases cutting feed increases. As the cutting feed increases, pressure also varies. There is a variation between pressure and SOD when SOD increases, pressure decreases. It is perceived that the most governing factor is cutting feed among all control factors.

Contour plot analysis for MRR

Figure 8a-c indicates the interaction effect of two parameters with respect to MRR are graphically represented using 3D contour plots. Figure 8a shows standoff distance versus cutting feed when Pressure is set to the middle value of 49.642Mpa. Material removal rate increases as standoff distance decreases and cutting feed increases. Similarly, MRR decreases with increasing Standoff distance and decreasing cutting feed. The driving force of particles impacting with the workpiece reduces as the standoff distance rises, resulting in uneven peaks on the machined surface. In Figure 8b Cutting feed is shown versus Pressure by keeping Standoff distance as constant at 1.5mm. When the pressure is high and the cutting feed is low, the MRR decreases, and vice versa. In Figure 8c shows the combination of Pressure and SOD at constant Cutting feed 36.46 (mm/min). Minimum MRR is observed at lower SOD and higher pressure and vice versa.

Figure 8 only with higher CF material removal rate is influenced (8a) with higher feed increased material removal rate can be seen Figure 8b.

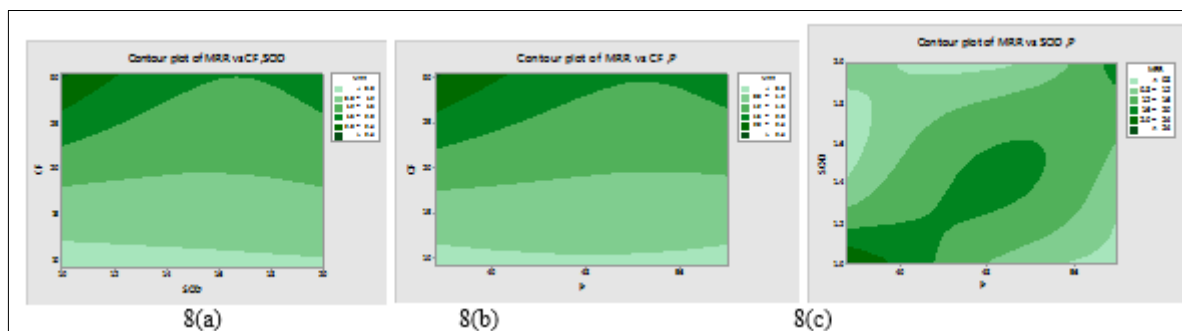


Figure 8a-c. Contour plots for MRR with Respect to input parameters

Figure 9 depicts the MRR residual plot with the Normal probability plot, Residual versus fits, histogram versus residuals, and residuals versus experimental values. The graph indicates that the measured and estimated values have a good relationship. The residual information is represented as a histogram. Experimental data vs. residual data, which is scattered between the zero and nonzero lines.

It is also seen that a reduction in material removal rate is associated with a rise in roughness. Unlike the case of conventional chip removal cutting process a reduction in material removal rate for water jet cutting could be associated with roughened texture possibly due to partial material removal.

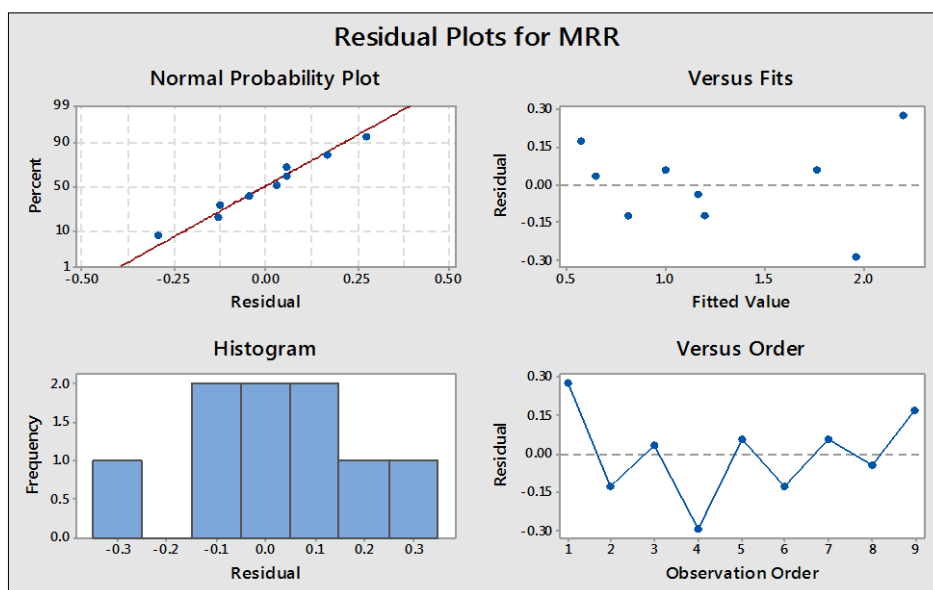


Figure 9. Residual plots for MRR

3.3. RSM optimization

The optimization plot depicts the effects of the variables on the predicted answers. Each variable is represented by a column in the optimization. The top row displays the composite desirability. A row for each response variable is given below the composite desirability. Cells indicate how one of the factors affects the related response variable or composite desirability, while the other variables remain constant [17].

The predicted response (y) at the current variable settings and the individual desirability score are shown to the left of each response row. The composite desirability (D) is shown in the top row and upper left corner. The used parameters are represented by vertical red lines on the graph. The current response values are represented by horizontal blue lines. Grey areas denote areas where the matching response is undesirable. RSM desirability function is used for optimization of response factors (SR, MRR). In the desirability technique, all response values are converted into a non-dimensional desirability value (d) that ranges from 0 to 1.

Table 8. RSM-optimized range of AWJM machining parameters

Input parameter/Response	Goal	Lower Limit	Upper Limit
Standoff distance (mm)	In range	1	2
Cutting Feed (mm/min)	In range	9.15	30.60
Pressure (Mpa)	In range	35.163	59.984
Surface Roughness(μm)	Minimize	1.993	2.493
Material removal rate(MRR)	Maximize	0.6805	2.4779

Response optimization plot: In Figure 10 optimization plot shows the variable effects of the predicted responses. The composite desirability of these two responses is 0.8583 [1, 17]. From the optimization plot it predicts that SOD (1mm), CF (30.60 mm/min), P (35.163Mpa) is chosen for machining of pockets. Using the optimal input parameters identified in the previous section, pocket milling was carried out on AISI 1045 material using Abrasive water Jet machine. Three geometries were machined; square, rectangle, and a circle. As complex geometries can be machined with a combination of these shapes, they were selected. The pocket dimensions are specified in Table 9.

Table 9. Pocket dimensions

S. No.	Shape	Dimensions
1	Square	15mm*15mm
2	Rectangle	30mm*15mm
3	Circle	ø 22mm

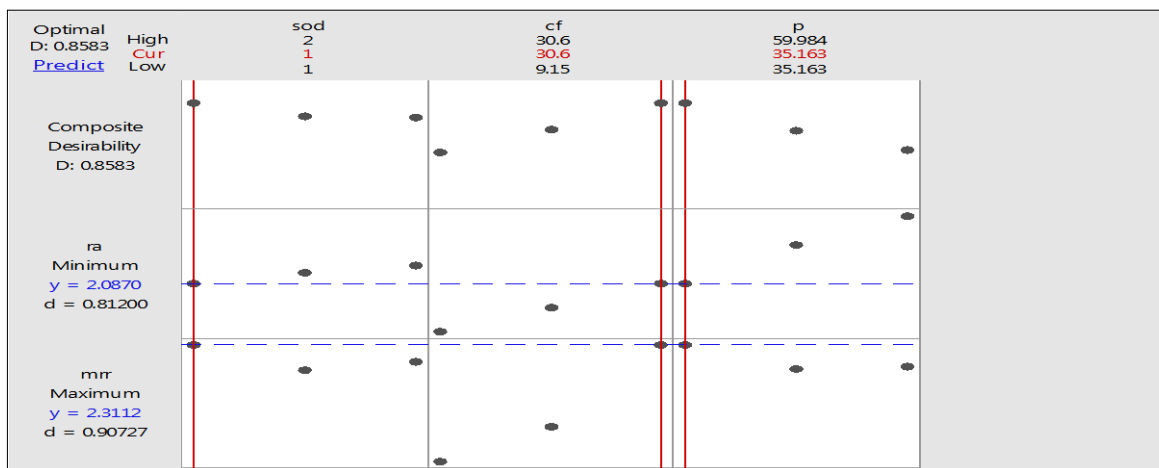


Figure 10. Response optimization plot

The MRR and SR for the work pieces are listed in Table 10.

Table 10. MRR and SR for each wrk piece

S. No.	Shape	Machining time, min	Mass of material removed, g	SR, μm	Abrasive Qty	MRR, mm^3/min
1	Square	1.402	4.820	2.33	0.48 kg	3.4379
2	Rectangular	2.757	9.692	2.24	0.97 kg	3.5154
3	Circle	1.543	4.886	2.28	0.53 kg	3.1665

The pocket depth for each workpiece and tool path transverse length are tabulated in Table 11.

Table 11. Pocket Depth and Tool path travel length

S. No.	Shape	Pocket Depth, mm	Travel length, mm
1	Suare	2.74	600.20
2	Rectangular	2.82	1216.00
3	Circle	1.63	788.16

A raster tool path with an overlap of 75% is considered. This overlap has experimentally proven to reduce surface roughness [5,7]. The machine's traverse rate slows down in locations where the jet changes direction due to the machine's dynamics. Because of the aforementioned occurrence, the depth at the corners is significantly increased as a result of this deceleration.

4. Conclusions

The current research examines the influence of various process parameters on response parameters when machining AISI 1045 steel. For assess the significance of the proposed model, Taguchi and ANOVA are utilised. Multi-objective RSM technique Response optimization plot is used to draw the required results.

The most significant parameter for surface roughness is pressure, while the most significant parameter for material removal rate is cutting feed.



Surface roughness and Material Removal Rate have mean absolute errors (MSE) of 0.04 and 0.27, respectively. Also, R^2 and R^2 adj values for surface roughness and MRR are 89.44;83.11 and 92.60; 87.68 % respectively. As a result, there is a strong correlation between experimental and anticipated results.

The Main effect plot and the 3D contour analysis plots are used for analyze the effects of process parameters. Standoff distance is comparatively less significant than Cutting feed and Pressure.

The Optimum values of SOD, CF, and P are 1mm, 30.60 mm/min, 35.163 Mpa respectively. Multi-objective optimization using RSM is used to minimize surface roughness and maximize MRR, yielding a composite desirability of 0.8583.

The confirmation test is run with the best values that yielded the best results. Pockets of different shapes were machined successfully using Transverse path with an overlap of 75%. Pockets were machined to a depth of 2.82mm approximately. Experimental and predicted values are correlated. Future work can be done on changing the tool path strategies, Optimization of power consumption.

References

1. PARIKSHIT A. DUMHARE, SHIKHA DUBEY, YOGESH V. DESHPANDE (2018), Modeling and multi-objective optimization of surface roughness and Kerf taper angle in abrasive water jet machining. *Journal of the Brazilian Society of Mechanical Sciences and Engineering* **40**: 259.
2. VAN HUNG BUI, PATRICK GILLES, TAREK SULTAN, GUILLAUME COHEN., 2017, A new cutting depth model with rapid calibration in abrasive water jet machining of titanium alloy. *International journal of manufacturing Technology* **93**:1449-1512.
3. SUDHAKARR.LOHAR., PRAVIN R. KUBAE., 2017, Investigation of effect of Abrasive water jet machining process parameters on performance characteristics of High carbon High chromium Steel. *International Advanced Research Journal in science, Engineering and Technology*, 2393-8021.
4. D.D. PATEL, HARDIKKUMARRASIKALDODIYA, D.L. LALWANI., 2016, Experimental investigation of CNC machining of elliptical pockets on AISI 304 stainless steel. *Int.J. Experimental Design and Process Optimization*, Vol. **5**, Nos.1/2.
5. U.GOWTH A.M., BASAWARAJ.S.HASU, G. CHAKRAVERTI, M. KANTHABABU., 2016, Experimental Investigation of Pocket milling on Inconel 825 using Abrasive water jet machining. *International Journal of current Engineering and Technology*, 2277-4106.
6. Y. AHED, C. ROBERT, G. GERMAIN, A. AMAR., 2016, Development of a numerical model for the understanding of the chip formation in high-pressure water jet assisted machining. *Finite element in analysis and Design* **108**, 1-8.
7. T.V.K. GUPTA, J. RAM KUMAR, PUNEETTANDON, N.S. VYAS., 2013, Role of process parameters on Pocket milling with Abrasive Water jet Machining Technique. *International Journal of Mechanical and Mechatronics Engineering* vol:**7**, No.10.
8. DEBASISH GHOSH, PROBALK DAS, B. DOLOI., 2014. Parametric studies of abrasive water jet cutting on surface roughness of silicon nitride materials. *All India Manufacturing Technology, Design and Research Conference*, IIT Guwahati, Assam, India.
9. NARESH KUMAR, MUKULSHUKLA., 2012, Finite element analysis of multi - particle impact on erosion in abrasive water jet machining of titanium alloy. *Journal of computational and applied Mathematics* **236**, 4600-4610.
10. ANKUSH SHARMA, D.I. LALWANI., 2013, Experimental investigation of process parameters influence on surface roughness in abrasive water jet machining of AISI H13 die steel. *Proceedings of conference on Intelligent, Robotics, Automation and Manufacturing* 333-341.
11. M. KANTHABABU, O.V. KRISHNAIAHCHETTY., 2003, A study on recycling of abrasives in abrasive water jet machining *Wear* **254**, 763-773.
12. P. SITARAMA CHAKRAVARTHY, N. RAMESH BABU., 2000, A hybrid approach for selection of optimal process parameters in abrasive water jet cutting. *ProcInstnMechEngrs* Vol **214** Part B 781-791.

- 13.S. PAUL, A.M HOOGSTRATE, C.A. VANLUTTERVELT, H.J.J. KALS., 1998. An Experimental investigation of Rectangular pocket milling with abrasive water jet machining. *Journal of Materials Processing Technology* **73**, 179-188.
- 14.J. WANG, W.C.K. WONG., 1999. A Study of abrasive water jet cutting of metallic coated sheet steels *International Journal of Machine Tools & Manufacture* **39**, 855-870.
- 15.G. A. ESCOBAR-PALAFIX, R.S GAULT, K RIDGWAY., 2012, Characterization of abrasive water-jet process for pocket milling in Inconel718 *Procedia CIRP* **1**, 404-408.
- 16.POPAN A., BALC N., CAREN A., LUCA A., MIRON A., 2015, Research on Abrasive water jet milling of the planar surfaces, slots and profiles *Applied mechanics and materials*, Vol. **760**, 409-414.
- 17.BHASKAR GOVINDASAMY BHAVANI, GURU PRASATHMUTHUKRISHANAN YOGA, MOHANA SUNDARAMRAMASUBRAMANIA, ARUN KUMARR BALAJI, SELVA KUMAR MARIAPPAN, LENIN RAJ SUNDARAJAN, VARATHARAJAN RAJAGOPALAN., 2018. AN EXPERIMENTAL STUDY ON DEEP HOLE MACHINING IN BRASS USING ABRASIVE WATER JET MACHINE, *International Journal of ModernManufacturing Technologies*, published by Professional Association in Modern ManufacturingT. Vol. **10**, Issue 1, pp. 27-36.
- 18.M. KANTHA BABU, RAJES RAM M, PETER NITHINEMANNUEL, R GOKUL, RADHIKRAMMOHAN., 2016, Experimental investigations on pocket milling of titanium alloy using abrasive water jet machining *FME transactions* **44**, 133-138.

Manuscript received: 31.12.2021